Colloidal Apatite Nanoparticles Exhibiting Luminescence and Magnetic Susceptibility

A. Nickel*, K.H. Prakash**, M. Pedulla* and R. Kumar*

*Montana Tech of the University of Montana, MT, Butte, USA, rkasinath@mtech.edu
**University of Queensland, Brisbane, Australia, prakashkithva@yahoo.com.sg

ABSTRACT

It is inherently difficult to synthesize colloidally dispersed nano-hydroxyapatite (nHA) particles and perhaps create primary nHA building blocks that can be utilized for bottom-up assembly, potentially making them even more attractive candidates for drug and gene delivery systems. This work presents an effective way to synthesize highly dispersed colloidal nHA particles by controlled aging of a calcium phosphate gel in conjunction with citrate molecules. A range of multi-functional traits (e.g. magnetic and luminescent behavior) is demonstrated by doping the apatite lattice in situ with Fe(III) ions. The as-synthesized suspensions (2g/L) consisted of 10 nm equiaxed primary nHA particles. Controls settled within 30 minutes, while nHA suspensions stabilized with citrate groups exhibited colloidal stability for months. XRD and Rietveld refinement revealed structural changes and FTIR spectroscopy traced the evolution of the precursor compounds into nHA particulates. In effect, the work demonstrates the possibility to synthesize multi-functional nHA for bio-medical applications.

Keywords: apatite, nanoparticles, multifunctional, synthesis

1 INTRODUCTION

Several levels of functionality, in biological processes, are achieved through rudimentary bio-molecules such as proteins and polysaccharides, which are usually in nanometer dimensions [1]. Ideally, this enables the use of nanoparticles (5-50 nm) to probe, for example cellular processes at those size scales. Designed nanoparticles intended for use in biotechnology are generally classified under a broad umbrella of materials called nano-biomaterials. Organic molecules, adsorbed on the surface of the nanoparticle can be used to control size. However, the same layer might also serve as a linker, facilitating the binding of various biocompatible moieties depending on the function required by the specific application. However, there needs to be, other than size not to mention minimal toxicity, three other important qualities that nanoparticles need to possess before they can be effectively utilized for these applications. (1) The *potential for interaction* between the nanoparticle and its intended target. This is typically achieved through surface modifications that would illicit binding with an antibody, or cell-receptor complements attached via a linker or a monolayer of small molecules, [2,3] (2) *Easy particle tracking and detection*. This implies the particle needs to exhibit fluorescent behavior (emission ideally being in visual range) or the ability to detectably change optical properties easily, and (3) *Easy manipulation*, e.g., "magnetic" nanoparticles that can be guided to the target with the use of an external magnetic field. This also suggests that the nanoparticles should ideally exhibit super-paramagnetic properties, characterized by high magnetic saturation and minimal or no remenance as compared to ferromagnetic materials [4 and references therein]. The combination of these characteristics coupled with suitable particle size tuned for the application make nanoparticles highly versatile for a large number of biological and other applications. Ideally, the combination of selectivity and tuned magnetic and luminescent properties results in the simultaneous ability to target, detect and manipulate nanoparticles. However, at present, the ability to produce un-agglomerated individualized nanoparticles below 50 nm is still a daunting task. In this work we demonstrate the synthesis of 10 nm equiaxed dispersions of nHA particles using wet chemistry that utilizes citrate groups to cap and stabilize HA nuclei during crystallization.

2 MATERIALS AND METHODS

2.1 Synthesis

Colloidally stable nHA was synthesized at 40°C using calcium hydroxide, $Ca(OH)_2$ and potassium di-hydrogen phosphate, KH_2PO_4 (both analytical grade from Sigma-Aldrich, USA). De-ionized (DI) water (Milli-Q unit, Millipore, USA) was used to prepare all the solutions/suspensions in the present study. To suspensions of 50 mmoles Ca(OH)2 in 200 ml of dH_2O (heated to 37º C), 0.5-3.5 mmoles of citric acid was added under constant stirring followed by 50 ml of 30 mmoles of KH_2PO_4 solutions. The resulting sol was sealed and stirred at 37º C for 7 days. The starting pH was roughly 9.5 and final pH was 7.6. Fe(III) doped apatites were synthesized by introducing the appropriate mole fractions of soluble $FeCl_3$ so as to achieve 10-40% Ca- atom substitution in the lattice.

2.2 Characterization

A Zeta potential particle analyzer (Malvern Instruments, USA) was used to measure the particle size. X-

ray diffraction was used to determine the crystal parameters and structural changes. The samples were scanned with Cu-K_α X-ray radiation from a Philips XRD 3720 at 40 kV and 20 mA, using a step size of 0.01° with a time of 2 sec/step, over a 2θ range of 20-50°. Preliminary quantitative analysis of the XRD data was carried out by Rietveld full profile fitting using the MAUD (Ver. 2.04) crystallographic refinement software, the details of which are reported elsewhere [5-7]. The XRD data was also refined to construct crystallite shape and size based on the Popa model [8]. Micrography samples were prepared by drying a concentrated drop onto an aluminum stub covered in double-sided copper tape. The samples were then analyzed using a 6330 JEOL FEG-SEM at 15kV. Morphology of the nanoparticles was also observed in a Hitachi Transmission Electron Microscope (TEM) at 100 KeV by pipetting 10µl of the as prepared suspension onto the copper grid and wicking off the access liquid after 30 seconds. Fourier Transform Infrared (FTIR) spectroscopy (Perkin-Elmer System 2000) was carried out to temporally investigate the structural evolution of the amorphous gel into nHA particles. Samples were prepared by isolating the gel/particles by centrifuging and washing the pellet twice. The pellet was then dried in a 70°C oven for two days, and mixed and ground with KBr homogeneously. An average of 100 scans at 2 cm^{-1} resolution was taken for each sample, between 400-4000 cm^{-1}, in the diffuse reflectance mode.

3 RESULTS AND DISCUSSION

After 3-4 days, at 2.5mmoles of citric acid, a highly stable dispersion of HA nanoparticles, totally transparent to the naked eye, was evident (Figure 1). FEM and TEM micrographs revealed that the stable suspensions consisted of equiaxed nHA primary particles roughly 10nm in size (Figure 2). TEM images revealed that the primary particles were aggregated into directional nanostructures.

Figure 1 As synthesized nHA nanoparticle dispersion (left) as compared to plain water (right). The dispersion were transparent enough to be undifferentiated with water.

It is well known that citrate groups chelate Ca^{2+} ions with high efficiency and suppress HA crystal nucleation and growth. We experimented with the possibility of trace amounts of citrate groups in the crystallization solution modulating the growth process and surface chemistry of HA nanoparticles. After 7 days, the suspension was still clear and transparent, and the final pH was about 7.6.

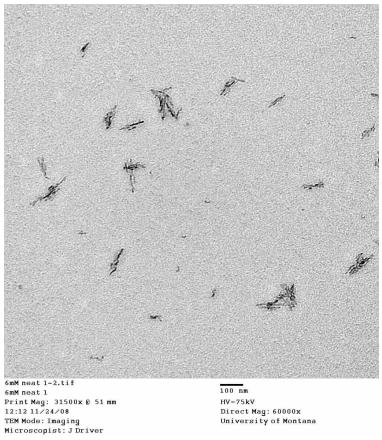

(a)

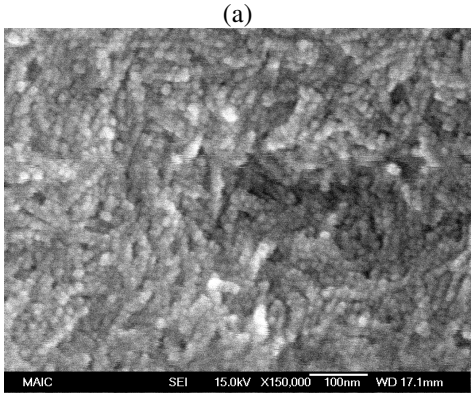

(b)

Table 1: Figure 2 (a) TEM micrograph showing the particle size and shape and (b) FEM micrograph indicating the possibility to produce controlled aggregation.

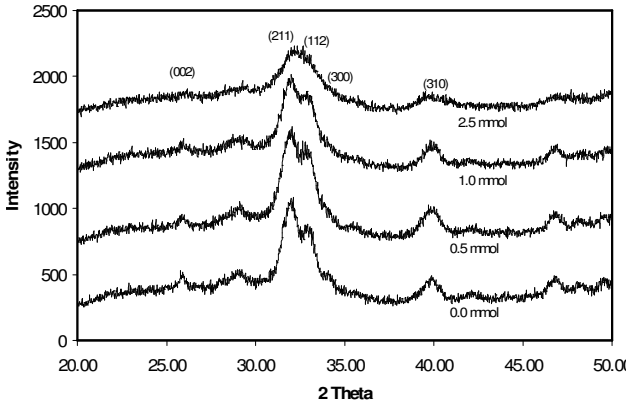

Figure 3 XRD of centrifuged nanoparticles prepared using citric acid at various concentrations. As the citric acid was increased the 002 peak was diminished and the 211, 112 and 300 peaks merged into one broad peak signifying a smaller particle size and possible higher sphericity.

NSTI-Nanotech 2009, www.nsti.org, ISBN 978-1-4398-1783-4 Vol. 2, 2009

As seen from the X-ray diffraction (XRD) experiments (Figure 3) there is a decrease in the (002) and (300) peak intensity with increasing citrate concentration. This coincides with a decrease in the aspect ratio of the particles as the citrate concentration increased. Increasing the citrate concentration beyond 7 mM (3.5 mmoles) was investigated, but the experiments resulted in amorphous gels which did not evolve to precipitate crystalline nanoparticles, even after aging for 2 weeks. Presumably this seems to be due to the high Ca^{2+} ion chelation capability of citrate groups. In the dried samples there was also an increase in the ordering of the particles as the citrate concentration was increased (Figures 2a-b). This increase in ordering could be due to the narrow size distribution and increase in surface functionality by citrate groups the mono-, bi-, or tri-dentate forms. Rietveld refinement results revealed that the crystal parameters were close to standard HA samples. Considering that the lattice parameters of HA is roughly 9.42 and 6.88Å, it is rather remarkable that these particles probably contain only about 8-10 unit cells in the a-b axis and 6-7 in the c axis (total of 380-700 unit cells). XRD also indicated a decrease in average crystallite size as a function of increasing citrate concentration.

FTIR spectrums tracing the evolution of the starting gel into the precipitated particles are shown in Figure 4. The results indicated that the starting precursor gel had a roughly amorphous character given the presence deformation bands of free-phosphate, which then evolved into phosphate bands corresponding to v1, v3 and v4 deformation bands in the apatite lattice.

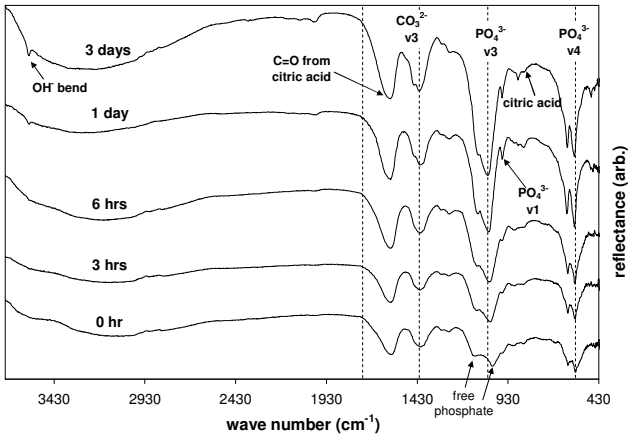

Figure 4 FTIR spectrums indicating the gradual evolution of the free phosphate bands into those corresponding to wavenumbers of phosphate bands in hydroxyapatite.

The exact details of the mechanism leading to this particulate size, distribution and colloidal behavior for HA are, however, yet to be determined. However, assuming the citric acid forms a monolayer around the particles and based on the known head area of 1 citrate molecule being 22 x 10^{-20} m^2, the weight of citric acid per particle can be calculated comparing the surface area of the particle and 1 head group as $[(\pi dp^2/a) \times (M/N_0)]$, where d_p is the particle diameter (10 nm), a is head area per citrate molecule = 22 x 10^{-20} m^2), M is the mass/mole = 192 g/mol and N_o is the Avogadro's number or 6.022 x 10^{23} molecules/mol. This leads to about 4.5 x 10^{-19} g of citrate molecules per particle.

Generally, this work suggests that the citrate groups might serve two functions. It seems to, firstly, cap the HA nuclei and restrict nanoparticulate growth in equilibrium growth axis (c-axis). Secondly, by binding to these nanoparticles, it presumably gives the particle surface a net negative charge resulting in the observed colloidal stability. In order to investigate this phenomenon in detail, separate studies incorporating other carboxylic acids under different conditions (pH, ionic strength and temperature) needs to be carried out. However, our current perception, from the size of the particles and their prolonged stability at physiological pH, is that they would be ideal candidates as viable carriers or complex formers with DNA for gene delivery [8].

This wet chemical route also seems amicable for the convenient doping of stable nHA particles. This was carried out by adding 10-40 mol % of Fe (in the form of a soluble salt), with respect to calcium in apatite during the original synthesis experiment. The experiments revealed that the technique was feasible for synthesizing Fe-doped apatite particles and even other metal-ion doped varieties (not shown here). The Fe-doped HA nanoparticles too maintained colloidally stability for weeks, but were not as stable as the neat nHA particles. This could be due to the increasing ionic strength of the solution (with the addition of dopant salts) decreasing colloidal stability. The Fe-doped particulates revealed novel characteristics as seen from their magnetic and luminescent behavior. Figure 5 reveals the green luminescence of a Fe-doped nHA suspension when exposed to ultra-violet (UV) light. This preliminary observation indicated that the Fe-doped apatites could be excited by UV radiation and emitted green light. The absorbance profile of Fe-doped HA nanoparticles revealed an absorbance peak at about 260 nm, not present in the un-doped samples (not shown here), corroborated this possibility to some extent.

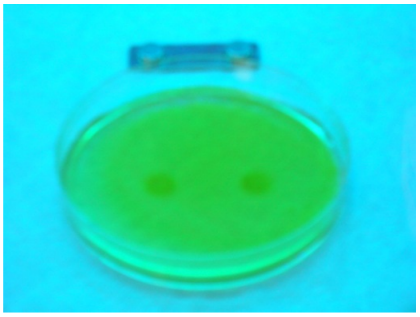

Figure 5 Fe-doped nHA suspension exhibiting green fluorescence when exposed to UV radiation.

Figure 6 illustrates the magnetic field assisted assembly of 40 mol % Fe-doped HA particles. Small Nd-

Fe-B magnets were assembled to pattern the letters “M T”. The Fe-HA colloidal suspension was then poured in a Petri dish, and placed on top of this pattern. After 2 hours the nanoparticles were seen to specifically aggregate only over the regions delineated by the magnets. Considering that the magnets used were relatively weak (~ 0.1 Tesla) the aggregation (writing) behavior appeared to be remarkable. Furthermore, upon removal of the magnet and slight agitation the colloidal state was regained, perhaps hinting on the possibility of super-paramagnetic properties.

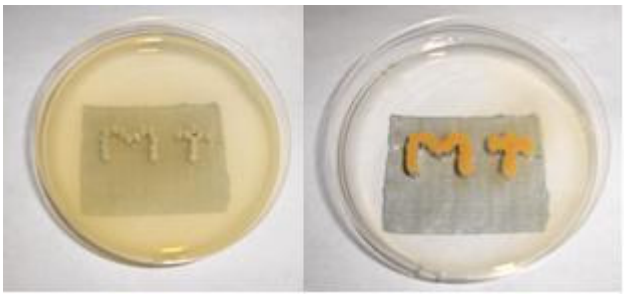

Figure 6 Photographs showing the possibility to assemble magnetically susceptible Fe-doped nHA particles with the assistance of external magnetic fields.

4 CONCLUTIONS

This study has revealed the possibility to synthesize colloidally dispersed nHA particles through a simple wet chemical technique. This technique seems ideal for HA, as it sufficiently retards the formation of equilibrium shaped acicular HA particles simultaneously creating a stable colloid. Additionally, this synthesis route has the added advantage to introduce impurity atoms into the apatite crystal lattice employing virtually any metal dopant. These dopants can be used to tailor the physical and chemical properties of HA resulting in multifunctional nanoparticles exhibiting luminescence and magnetic enhancements. With the ability to disperse and dope monocrystalline apatite nanoparticles with Fe and maybe a variety of metal ions, we are could tailor intrinsic properties of these apatite nanoparticles and perhaps synthesize nHA particles which exhibit superconducting, superparamagnetic, fluorescent, photo-catalytic, anti-bacterial and perhaps other yet to be revealed properties.

REFERENCES

[1] Salata, O. V., Applications of nanoparticles in biology and medicine. Journal of Nanobiotechnology , 2004, 2.

[2] Sinani, V. A.; Koktysh, D. S.; Yun, B. G.; Matts, R. L.; Pappas, T. C.; Motamedi, M.; Thomas, S. N.; Kotov, N. A., Collagen coating promotes biocompatibility of semiconductor nanoparticles in stratified LBL films. Nano Letters 2003, 3 (9), 1177-1182.

[3] Zhang, Y.; Kohler, N.; Zhang, M., Surface modification of superparamagnetic magnetite nanoparticles and their intracellular uptake. Biomaterials 2002, 23 (7), 1553-1561.

[4] Sugunan, A.; Melin, P.; Schnurer, J.; Hilborn, J. G.; Dutta, J., Nutrition-driven assembly of colloidal nanoparticles: Growing fungi assemble gold nanoparticles as microwires. Advanced Materials 2007, 19 (1), 77-81.

[5] Kumar, R.; Cheang, P.; Khor, K. A., Phase composition and heat of crystallisation of amorphous calcium phosphate in ultra-fine radio frequency suspension plasma sprayed hydroxyapatite powders. Acta Materialia 2004, 52 (5), 1171-1181.

[6] Kumar, R.; Prakash, K. H.; Cheang, P.; Khor, K. A., Microstructure and mechanical properties of spark plasma sintered zirconia-hydroxyapatite nano-composite powders. Acta Materialia 2005, 53 (8), 2327-2335.

[7] McCusker, L. B.; Von Dreele, R. B.; Cox, D. E.; Louer, D.; Scardi, P., Rietveld refinement guidelines. Journal of Applied Crystallography 1999, 32, 36-50.

[8] Popa, N. C., The (hkl) dependence of diffraction-line broadening caused by strain and size for all Laue groups in Rietveld refinement. Journal of Applied Crystallography 1998, 31, 176-180.

[9] Kumar, R.; Chew, M.; Lim, Y.; Kiat, N. H.; Kueh, J.; Cheang, P.; Khor, M.; Man, H. K., Nano bio-ceramic vectors for non-viral transfection. Cancer Gene Therapy 2004, 11 (12), 854-854.